

Chromomagnetic Instability and Gluonic Phase at Nonzero Temperature

O. Kiriyaama

Institut für Theoretische Physik, J.W. Goethe-Universität, D-60438 Frankfurt/Main, Germany

Abstract. We describe the results of recent studies of a chromomagnetic instability and a gluonic phase in neutral two-flavor quark matter at nonzero temperature.

Keywords: Quark matter, Color superconductivity, Chromomagnetic instability, Gluonic phase

PACS: 12.38.-t, 11.30.Qc, 26.60.+c

INTRODUCTION

Sufficiently cold and dense quark matter is a color superconductor. Color superconducting phases at “moderate” density, which is relevant for quark matter in the interior of compact stars, have a rich phase structure and have recently attracted a great deal of interest [1].

Bulk matter in the interior of compact stars should be in β -equilibrium and be neutral with respect to electric and color charges. In the two-flavor case, these conditions separate the Fermi momenta of up and down quarks and, as a consequence, the ordinary BCS state (2SC) is not always energetically favored over other unconventional states, e.g., the gapless two-flavor color superconductivity (g2SC) [2]. However, the 2SC/g2SC phases suffer from a chromomagnetic instability, indicated by imaginary Meissner masses of some gluons [3]. The instability related to gluons of color 4–7 occurs when the ratio of the gap over the chemical potential mismatch, $\Delta/\delta\mu$, decreases below a value $\sqrt{2}$. Resolving the chromomagnetic instability and clarifying the nature of the true ground state of dense quark matter are central issues in the study of color superconductivity [4, 5, 6, 7, 8, 9, 10, 11, 12, 13, 14, 15, 16, 17, 18, 19, 20].

So far, several candidates for the ground state have been proposed [4, 5, 6, 7, 8, 9, 18]. In this work, we study the gluonic phase (gluonic cylindrical phase II) [9] at nonzero temperature.

FREE ENERGY OF GLUONIC PHASE

Model

In order to study the gluonic phase, we use a gauged Nambu–Jona-Lasinio model with massless up and down quarks:

$$\mathcal{L} = \bar{\psi}(i\not{D} + \hat{\mu}\gamma^0)\psi + G_D \left(\bar{\psi}i\gamma_5\epsilon\epsilon^b C\bar{\psi}^T \right) \left(\psi C i\gamma_5\epsilon\epsilon^b \psi \right) - \frac{1}{4}F_{\mu\nu}^a F^{a\mu\nu}, \quad (1)$$

where the quark field ψ carries flavor ($i, j = 1, \dots, N_f$ with $N_f = 2$) and color ($\alpha, \beta = 1, \dots, N_c$ with $N_c = 3$) indices, C is the charge conjugation matrix; $(\varepsilon)^{ik} = \varepsilon^{ik}$ and $(\varepsilon^b)^{\alpha\beta} = \varepsilon^{b\alpha\beta}$ are the antisymmetric tensors in flavor and color spaces, respectively. The diquark coupling strength in the scalar ($J^P = 0^+$) color-antitriplet channel is denoted by G_D . The covariant derivative and the field strength tensor are defined as

$$D_\mu = \partial_\mu - igA_\mu^a T^a, \quad F_{\mu\nu}^a = \partial_\mu A_\nu^a - \partial_\nu A_\mu^a + gf^{abc} A_\mu^b A_\nu^c. \quad (2)$$

The elements of the diagonal matrix of quark chemical potentials $\hat{\mu}$ in β -equilibrated neutral two-flavor quark matter are given by

$$\begin{aligned} \mu_{ur} = \mu_{ug} = \bar{\mu} - \delta\mu, \quad \mu_{dr} = \mu_{dg} = \bar{\mu} + \delta\mu, \\ \mu_{ub} = \bar{\mu} - \delta\mu - \mu_8, \quad \mu_{db} = \bar{\mu} + \delta\mu - \mu_8, \end{aligned} \quad (3)$$

with

$$\bar{\mu} = \mu - \frac{\delta\mu}{3} + \frac{\mu_8}{3}, \quad \delta\mu = \frac{\mu_e}{2}. \quad (4)$$

In Nambu-Gor'kov space, the inverse full quark propagator $S^{-1}(p)$ is written as

$$S^{-1}(p) = \begin{pmatrix} (S_0^+)^{-1} & \Phi^- \\ \Phi^+ & (S_0^-)^{-1} \end{pmatrix}, \quad (5)$$

with

$$(S_0^+)^{-1} = \gamma^\mu p_\mu + (\bar{\mu} - \delta\mu \tau^3) \gamma^0 + g\gamma^\mu A_\mu^a T^a, \quad (6)$$

$$(S_0^-)^{-1} = \gamma^\mu p_\mu - (\bar{\mu} - \delta\mu \tau^3) \gamma^0 - g\gamma^\mu A_\mu^a T^{aT}, \quad (7)$$

and

$$\Phi^- = -i\varepsilon\varepsilon^b \gamma_5 \Delta, \quad \Phi^+ = -i\varepsilon\varepsilon^b \gamma_5 \Delta. \quad (8)$$

Here $\tau^3 = \text{diag}(1, -1)$ is a matrix in flavor space.

For the gluonic phase, $B = \langle gA_z^6 \rangle$ is the most relevant vector condensate, because the tachyonic mode related to gluons 4–7 exists in the direction of B [9, 14]. Besides B , to ensure color neutrality at $B \neq 0$ we have to introduce $\mu_3 = \langle gA_0^3 \rangle$ [9]. In what follows, however, we neglect color chemical potentials μ_8 and μ_3 , since their effect on the free energy is negligibly small for $\alpha_s \simeq 1$. Taking account of B , the free energy of the gluonic phase in the one-loop approximation is given by

$$\begin{aligned} \Omega(\Delta, \mu_e, B; \mu, T) = & -\frac{1}{12\pi^2} \left(\mu_e^4 + 2\pi^2 T^2 \mu_e^2 + \frac{7\pi^4}{15} T^4 \right) \\ & + \frac{\Delta^2}{4G_D} - \frac{1}{2} \sum_a \int \frac{d^3p}{(2\pi)^3} \left[|\varepsilon_a| + 2T \ln(1 + e^{-\beta|\varepsilon_a|}) \right], \end{aligned} \quad (9)$$

where $\beta = 1/T$, the ε_a 's are quasi-quark energies and the sum runs over all particle and anti-particle ε_a 's. Note that the ε_a 's depend on B through the covariant derivatives in the

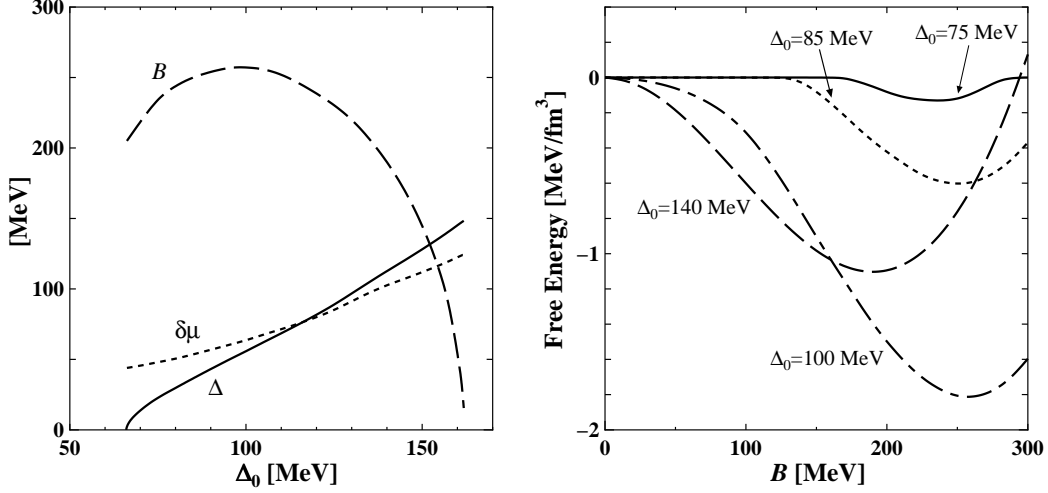


FIGURE 1. Left: The Δ_0 dependence of the gap Δ , the chemical potential mismatch $\delta\mu$, and the vector condensate B at $T = 0$. Right: The free energy (measured with respect to the 2SC/g2SC/NQ phases) as a function of B at $T = 0$. The results are plotted for $\mu = 400$ MeV.

quark propagator. Here, we added a contribution from electrons (first line on the r.h.s.). In order to evaluate loop diagrams we use a three-momentum cutoff $\Lambda = 653.3$ MeV throughout this work. In addition, in order to remove a cutoff dependence of the free energy we introduce the following subtraction:

$$\Omega_R = \Omega(\Delta, \delta\mu, B; \mu, T) - \Omega(0, 0, B; 0, 0). \quad (10)$$

Note that this free energy subtraction is not adequate to remove the cutoff dependence of the free energy at $T > 0$ [15]. However, we have carefully checked that it is nothing but a cutoff artifact and moreover is negligibly small at $\mu \sim 400$ MeV and at temperatures of interest (20 MeV at most). In order to find the gluonic phase, we first solve a set of coupled equations,

$$\frac{\partial \Omega_R}{\partial \Delta} = \frac{\partial \Omega_R}{\partial \delta\mu} = 0, \quad (11)$$

as a function of B and, then, compute $\Omega_R(B)$. Finally, the minimum of $\Omega_R(B)$ determines the gluonic phase.

Numerical results

In the left panel of Fig. 1, we plot Δ , $\delta\mu$ and B as a function of Δ_0 , the 2SC gap at $\delta\mu = 0$. (Essentially, Δ_0 corresponds to the diquark coupling strength.) We find that the gluonic phase exists in the window $66 \text{ MeV} < \Delta_0 < 162 \text{ MeV}$ and that a strongly (weakly) first-order transition between the gluonic phase and the NQ (2SC) phase takes place at $\Delta_0 = 66$ (162) MeV. Note that the results are consistent with those in Ref.

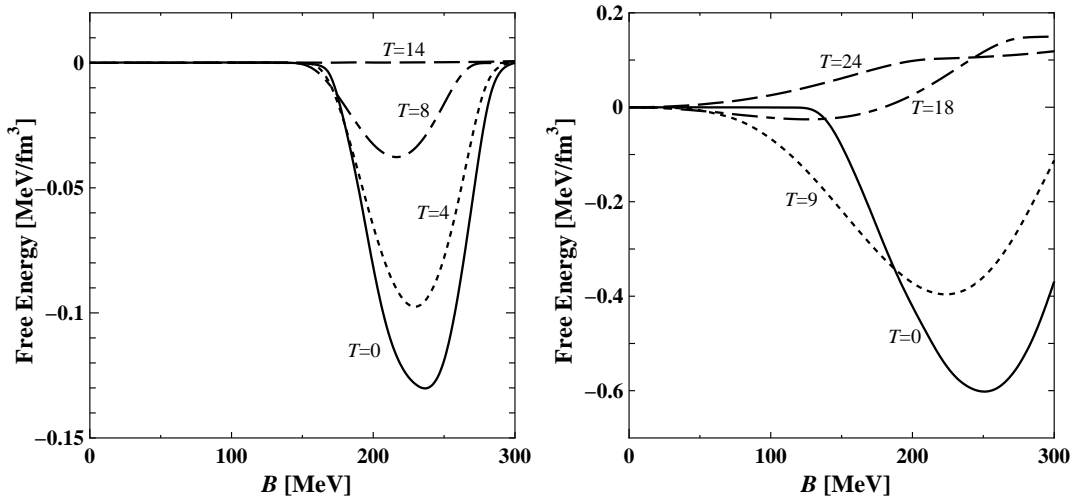


FIGURE 2. The temperature dependence of the free energy as a function of B for $\Delta_0 = 75$ MeV (left) and $\Delta_0 = 85$ MeV (right). The quark chemical potential is taken to be $\mu = 400$ MeV.

[19], where the color chemical potentials μ_3 and μ_8 were treated self-consistently. The right panel of Fig. 1 shows the free energy $\Omega_R(B)$ (measured with respect to the 2SC/g2SC/NQ phases at $B = 0$) as a function of B at $T = 0$. One can see that, in the cases of $\Delta_0 = 75, 85$ MeV, the gluonic phase is energetically more favored than the chromomagnetically stable NQ phase at $B = 0$. [For small values of B , we found that the system is in the ungapped phase and the free energy behaves like $\Omega_R(B) \sim O(B^4)$.] On the other hand, for $\Delta_0 = 100$ MeV and $\Delta_0 = 140$ MeV, the 2SC/g2SC phases at $B = 0$ are unstable and, then, the gluonic phase is energetically favored, as expected.

In Fig. 2, we plot the temperature dependence of the free energy for $\Delta_0 = 75$ MeV (left) and $\Delta_0 = 85$ MeV (right). At $\Delta_0 = 75$ MeV, the free energy gain gets rapidly reduced when T is increased, but the vacuum expectation value of B is only slightly reduced. Then we find a strongly first-order transition at $T \simeq 14$ MeV. In the case of $\Delta_0 = 85$ MeV, the gluonic phase is energetically more favored than the chromomagnetically stable NQ phase at low temperature. At $T \simeq 9$ MeV, the stable NQ phase undergoes a phase transition into the unstable g2SC phase. The gluonic phase is energetically favored over the unstable g2SC phases until the temperature reaches $T \simeq 20$ MeV. Above this temperature, the gapless dispersion relation is smoothed out and the stable g2SC phase is favored.

Here, we would like to make a comment regarding the order of the phase transitions. In the weak coupling regime, the transition from the gluonic phase to the NQ phase is strongly of first order. On the other hand, the phase transitions from the gluonic phase to the 2SC/g2SC phases in the intermediate coupling regime are likely to be of second order. However, evaluating the free energy near the critical temperatures self-consistently is not easy. Thus we cannot exclude the possibility of weakly first-order transitions.

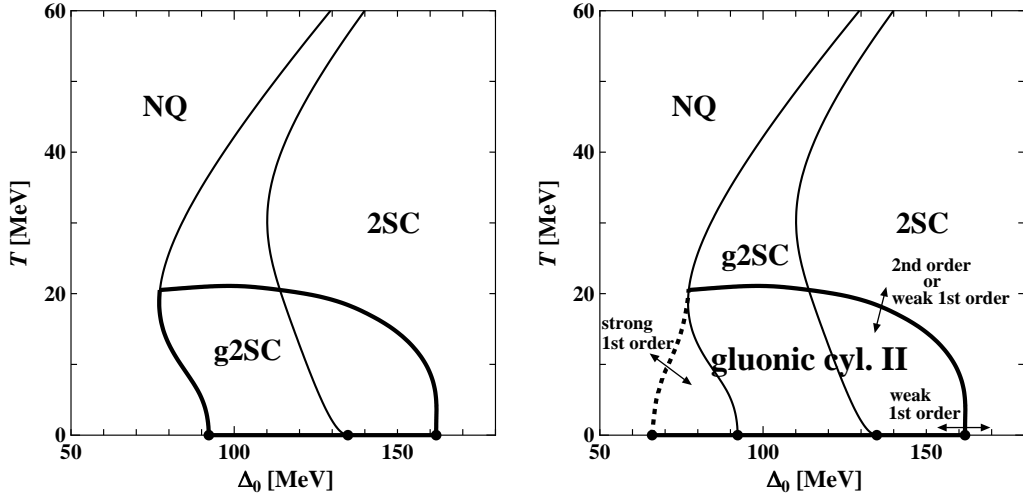


FIGURE 3. Left: The Δ_0 - T phase diagram of electrically neutral two-flavor quark matter. At $T = 0$, the g2SC phase exists in the window $92 \text{ MeV} < \Delta_0 < 134 \text{ MeV}$ and the 2SC window is given by $\Delta_0 > 134 \text{ MeV}$. The unstable region, where gluons 4–7 are tachyonic, is depicted by the region enclosed by the thick solid line. The g2SC phase and a part of the 2SC phase ($92 \text{ MeV} < \Delta_0 < 162 \text{ MeV}$) suffer from the chromomagnetic instability at $T = 0$. Right: Schematic phase diagram of the gluonic phase [20]. In the region enclosed by the thick solid and dotted lines, the gluonic phase is more favored than the 2SC/g2SC/NQ phases. First-order phase boundary is indicated by the thick dotted line. The thick solid line denotes the line of second-order or weakly first-order transitions.

CONCLUSION

In the left panel of Fig. 3, we plot the phase diagram of the electrically neutral 2SC/g2SC phases in the plane of Δ_0 versus T . The region enclosed by the thick solid line is unstable because the Meissner mass of gluons 4–7 is imaginary there. Note, however, that we did not examine the global structure of the free energy self-consistently. Therefore we should regard this result as the tendency toward the gluonic phase in the 2SC/g2SC phases. In fact, at $T = 0$, the gluonic cylindrical phase II exists in the wider window $66 \text{ MeV} < \Delta_0 < 162 \text{ MeV}$ (see also Ref. [19]).

In this work, we studied the phase structure of the gluonic cylindrical phase II at nonzero temperature. In the weak coupling regime, we found that the phase transition between the gluonic phase and the NQ phase is of strongly first order. In contrast, in the intermediate and strong coupling regimes, the transition is of second order or weakly first order. Therefore, in these regimes, the critical line shown in the left panel of Fig. 3 is not altered much by the self-consistent analysis. In the right panel of Fig. 3, we show the schematic phase diagram of the gluonic phase. One can see that the gluonic phase wins against a part of the NQ phase and enlarges its region. The phase transition to the NQ phase is of strongly first order (dotted line) while the transition to the 2SC/g2SC phases is of second order or weakly first order (solid line). The critical temperature for the gluonic phase is roughly given by $T_c \sim 20 \text{ MeV}$. (It is known that the gluonic phase survives until the temperature reaches $T_c \sim \delta\mu^{(\text{NQ})}/2$, where $\delta\mu^{(\text{NQ})}$ denotes the chemical potential mismatch in the NQ phase at $T = 0$ [15]. The present model

parameters yield $\delta\mu^{(\text{NQ})} \sim 40 \text{ MeV}$ and, hence, $T_c \sim 20 \text{ MeV}$.)

Finally, we comment on the outlook for future studies. Several candidates for the true ground state (for instance, other types of the gluonic phase [9] and a LOFF state with multiple plane waves [4]) have been proposed. It is then quite interesting to study the free energy of these phases and their stability against the chromomagnetic instability. In addition, since the gluonic phase dominates the low-temperature region of the phase diagram for the wide range of the coupling strength, it would have important implications for the properties of compact stars.

ACKNOWLEDGMENTS

I would like to thank Dirk Rischke for discussions. This work was supported by the Deutsche Forschungsgemeinschaft (DFG).

REFERENCES

1. K. Rajagopal and F. Wilczek, in *At the Frontier of Particle Physics/Handbook of QCD*, edited by M. Shifman (World Scientific, Singapore, 2001); M. G. Alford, *Annu. Rev. Nucl. Part. Sci.* **51**, 131 (2001); D. K. Hong, *Acta. Phys. Pol. B* **32**, 1253 (2001); S. Reddy, *Acta. Phys. Pol. B* **33**, 4101 (2002); D. H. Rischke, *Prog. Part. Nucl. Phys.* **52**, 197 (2004); R. Casalbuoni and G. Nardulli, *Rev. Mod. Phys.* **76**, 263 (2004); M. Buballa, *Phys. Rept.* **407**, 205 (2005); M. Huang, *Int. J. Mod. Phys. E* **14**, 675 (2005); I. A. Shovkovy, *Found. Phys.* **35**, 1309 (2005).
2. I. Shovkovy and M. Huang, *Phys. Lett. B* **564**, 205 (2003); M. Huang and I. Shovkovy, *Nucl. Phys. A* **729**, 835 (2003).
3. M. Huang and I.A. Shovkovy, *Phys. Rev. D* **70**, 051501(R) (2004); *Phys. Rev. D* **70**, 094030 (2004).
4. M. Alford, J. A. Bowers, and K. Rajagopal, *Phys. Rev. D* **63**, 074016 (2001); J. A. Bowers and K. Rajagopal, *Phys. Rev. D* **66**, 065002 (2002).
5. I. Giannakis and H. C. Ren, *Phys. Lett. B* **611**, 137 (2005); *Nucl. Phys. B* **723**, 255 (2005); I. Giannakis, D. f. Hou, and H. C. Ren, *Phys. Lett. B* **631**, 16 (2005).
6. S. Reddy and G. Rupak, *Phys. Rev. C* **71**, 025201 (2005); I. Shovkovy, M. Hanauske, and M. Huang, *Phys. Rev. D* **67**, 103004 (2005).
7. M. Huang, *Phys. Rev. D* **73**, 045007 (2006).
8. D. K. Hong, hep-ph/0506097.
9. E. V. Gorbar, M. Hashimoto, and V. A. Miransky, *Phys. Lett. B* **632**, 305 (2006); *Phys. Rev. D* **75**, 085012 (2007).
10. E. V. Gorbar, M. Hashimoto, and V. A. Miransky, *Phys. Rev. Lett.* **96**, 022005 (2006).
11. K. Fukushima, *Phys. Rev. D* **73**, 094016 (2006).
12. E. V. Gorbar, M. Hashimoto and V. A. Miransky, and I. A. Shovkovy, *Phys. Rev. D* **73**, 111502(R) (2006).
13. M. Hashimoto, *Phys. Lett. B* **642**, 93 (2006).
14. O. Kiriya, D. H. Rischke, and I. A. Shovkovy, *Phys. Lett. B* **643**, 331 (2006).
15. O. Kiriya, *Phys. Rev. D* **74**, 074019 (2006); *ibid.* **74**, 114011 (2006).
16. K. Iida and K. Fukushima, *Phys. Rev. D* **74**, 074020 (2006).
17. L. He, M. Jin, and P. Zhuang, *Phys. Rev. D* **75**, 036003 (2007).
18. R. Gatto and M. Ruggieri, *Phys. Rev. D* **75**, 114004 (2007).
19. M. Hashimoto and V. A. Miransky, *Prog. Theor. Phys.* **118**, 303 (2007).
20. O. Kiriya, arXiv:0709.1083 [hep-ph].